

**Poly(4-vinylphenol) coated magnetic nanoparticles based dispersive solid-phase  
microextraction of the determination of mercury(II) in water**

Abdulhadi Muftah Faraj Benrabha and Kheng Soo Tay\*

Department of Chemistry, Faculty of Science, University of Malaya, 50603 Kuala Lumpur,  
Malaysia

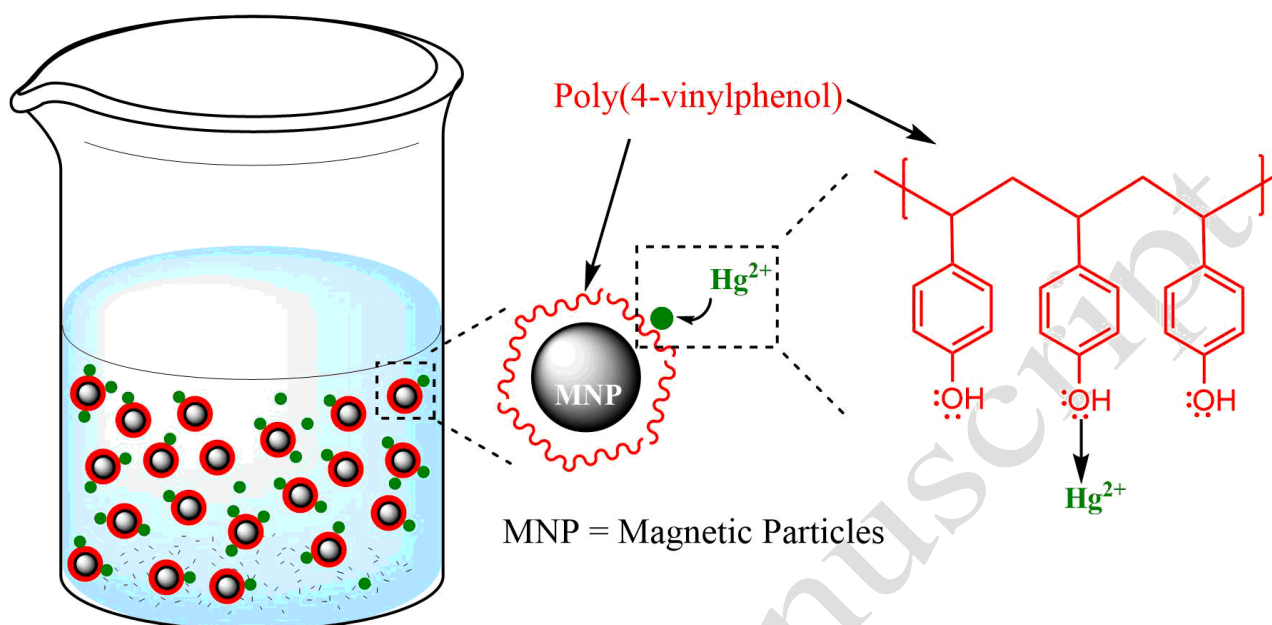
\*Corresponding author:

E-mail: khengsoo@um.edu.my, tel: +603-79677022 Ext 2145

accepted manuscript

## GRAPHICAL ABSTRACT

### Magnetic Dispersive Solid Phase Extraction of $\text{Hg}^{2+}$ using poly(4-vinylphenol) coated magnetic particles



## ABSTRACT

The development of magnetic sorbent for dispersive solid-phase micro-extraction (DmSPE) often requires lengthy multi-step reactions. This research revealed a simplified method for preparing magnetic sorbent for the DmSPE using poly(4-vinylphenol) (PVP). The magnetic sorbent (PVP@MNP) was prepared by coating PVP on magnetic particles (MNP). The characterization and formation of PVP@MNP were confirmed using infrared spectroscopy, scanning electron microscope, and energy-dispersive X-ray spectroscopy. The primary goal of this study is to develop a sensitive DmSPE method to analyze  $\text{Hg}^{2+}$  in water using PVP@MNP as a magnetic sorbent. The preparation of PVP@MNP was performed in a simple coating method at room temperature. Briefly, the PVP@MNP was prepared by sonicating the mixture of MNP and PVP. This sorbent was then used as a magnetic sorbent for the extraction of  $\text{Hg}^{2+}$  from water. The developed PVP@MNP based DmSPE reached a low method of detection limit ( $0.01 \mu\text{g L}^{-1}$ ) and limit of quantification ( $0.04 \mu\text{g L}^{-1}$ ). This method also showed a wide linearity range ( $100 - 2000 \mu\text{g L}^{-1}$ ) with a good correlation factor under optimized conditions. The developed method showed good recovery (72-90%) with good

intraday and interday precision. This study also showed that the developed DmSPE method was effectively used to determine  $\text{Hg}^{2+}$  in drinking water, mineral water, and surface water. The result also demonstrated that PVP@MNP is reusable.

**Keywords:** mercury (II) ion, magnetic particles, adsorption, removal mechanism, metal extraction, preconcentration

accepted manuscript

## 1. Introduction

The presence of heavy metals in water has become one of the most challenging environmental concerns (Shirani *et al.*, 2020). Although most of the heavy metals occurred in the water at trace level, it has been found to cause a toxic effect on living organisms due to its bioaccumulative behavior (Imran *et al.*, 2021, Marrugo-Negrete *et al.*, 2021). Among heavy metals, mercury (Hg) is known as toxic metal, which has been found to cause a wide range of adverse effects on the living organism (Dibbern *et al.*, 2021). Hg pollution has remained a major health concern. Therefore, rapid detection and analysis of Hg<sup>2+</sup> ions at trace levels are in critical need to protect those who are vulnerable (Pokhrel *et al.*, 2017).

Recently, dispersive micro solid-phase extraction (DmSPE) has gained much attention in sample preparation techniques because of its simplicity, speed, and efficiency (Chisvert *et al.*, 2019). This miniaturized sample preparation method involved the dispersion of a specific solid-phase or so-called sorbent in water matrices to extract targeted analytes. After extraction, the sorbent is often isolated via filtration or centrifugation. Then, the targeted analytes can be eluted from the sorbent using a specific reagent or solvent. The use of magnetic particles as sorbent has further simplified the DmSPE in sorbent isolation and elution. The magnetic sorbent can be isolated from water matrices using a magnet, and in this case, centrifugation is not required. The technique for the isolation of magnetic sorbent is more economical than the conventional sorbent without magnetic properties.

Bare magnetic Fe<sub>3</sub>O<sub>4</sub> is not suitable for being used as sorbent due to the poor surface properties to adsorb most of the analyte and easily oxidized characteristic. Consequently, research in this area has focused on developing new magnetic sorbents to enhance their efficiency, selectivity, physical and chemical stability (Chisvert *et al.*, 2019). Surface modification of magnetic particles with a ligand or specific chemical to enhance the adsorption of metal ions is one of the common methods to produce magnetic sorbent for DmSPE (Alinezhad *et al.*, 2020, Chen *et al.*, 2021, Ma *et al.*, 2020). This method often involves lengthy multi-step reactions, such as coating of magnetic particles, modifying the coated magnetic particles with a specific functional group or chemical, and the attached ligand (Fu *et*

*al.*, 2017). In this study, a simplified method was used to synthesize the poly(4-vinylphenol) (PVP) coated magnetic particles (PVP@MNP). PVP@MNP was used as a sorbent of DmSPE for the determination of  $\text{Hg}^{2+}$  in water. The application of PVP exhibits advantages that include insoluble in water, rapid and strong complexation with metals, low-cost and non-toxic nature (Zhang *et al.*, 2017). The coating of polymer on the magnetic particles could also enhance its stability during DmSPE by avoiding direct contact with the atmosphere. The objectives of this study were (1) to synthesize the PVP@MNP, (2) to study the behavior of PVP@MNP in removing  $\text{Hg}^{2+}$  from water, and (3) to develop a PVP@MNP based DmSPE method for the determination of  $\text{Hg}^{2+}$  in water. According to the literature search, the application of PVP@MNP as sorbent for DmSPE has not been reported.

## **2. Materials and methods**

### *2.1. Materials*

Iron (II) chloride tetrahydrate, ferric chloride hexahydrate, ammonium hydroxide solution (25%), HPLC grade isopropanol, sodium dihydrogen phosphate monohydrate, disodium hydrogen phosphate, and mercury standard solution (1000 ppm) were purchased from Merck (Germany). Poly(4-vinylphenol) was obtained from Sigma Aldrich. Ultrapure water was produced by using an Elga water purification system (UK). The Neodymium disc magnet (20 mm diameter  $\times$  3 mm height) was purchased from Eclipse Magnetics (UK). Drinking water and mineral water were purchased at a local market.

### *2.2. Synthesis of the MNP and PVP coated magnetic particles (PVP@MNP)*

Magnetic particle (MNP) was synthesized using the co-precipitation method at room temperature in the air (Khor *et al.*, 2019). Briefly, iron (II) chloride tetrahydrate and ferric chloride hexahydrate with a molar ratio of 2:3 were first dissolved in 50 mL deionized water in a beaker. Then 50 mL of ammonium hydroxide solution (25%) was added under stirring. The mixture was then stirred

vigorously for 30 min at room temperature. The obtained MNP was isolated using an external magnetic field, washed thoroughly with deionized water, and then vacuum dried.

For the synthesis of PVP@MNP, 0.5 g of MNP and 0.5 g of Poly(4-vinylphenol) (Sigma Aldrich) were added into the 50 mL isopropanol (Merck) in a conical flask. The mixture was sonicated for 30 min. The PVP@MNP were isolated from the isopropanol by using a neodymium magnet. The obtained PVP@MNP were rinsed thoroughly with deionized water and isopropanol. PVP@MNP was dried under vacuum and kept in a desiccator before being used.

### *2.3. Instrumentation for PVP@MNP characterization*

Perkin Elmer Spectrum 400 ATR-FTIR spectrophotometer was used to record the Fourier-transform infrared (FTIR) spectra. The resolution of  $2\text{ cm}^{-1}$  and 16 scans were applied to obtain the FTIR spectrum. The Scanning Electron Microscope equipped with Energy Dispersive X-ray (EDX) spectroscopy (Hitachi, SU8200) was used to capture the morphology of the MNP and PVP@MNP and determined the elemental composition.

### *2.4. Adsorption and kinetics studies*

To obtain an optimized method, the amount of adsorbent, adsorption time, the pH of the solution, and the initial concentration of  $\text{Hg}^{2+}$ , were optimized using one variable at a time method. The effect of operating parameters was evaluated by monitoring the percentage removal of  $\text{Hg}^{2+}$ . All experiments were performed in triplicate. The removal of  $\text{Hg}^{2+}$  by PVP@MNP was carried out in a 30 ml polypropylene bottle. For the adsorption study, 10 mg of PVP@MNP was added to the 20 mL of  $1\text{ mg L}^{-1}\text{ Hg}^{2+}$ . The mixture was shaken for the defined time interval. Then, the PVP@MNP was separated from the solution using the neodymium magnet. The remaining solution was sampled, and the concentration of  $\text{Hg}^{2+}$  was determined using a Mercury Analyzer (NIC RA-3).

The isolated adsorbent was washed with deionized water and vacuum dried. The isolated PVP@MNP was dispersed into a 0.5 mL of desorption reagent and shaken using the orbital shaker

for 5 min for the  $\text{Hg}^{2+}$  desorption. PVP@MNP was separated from the desorption reagent using a neodymium magnet placed at the outer part of the vial. The amount of  $\text{Hg}^{2+}$  in the desorption reagent was determined using Mercury Analyzer. The  $\text{Hg}^{2+}$  recovery calculated according to Equation (1):

$$\text{Recovery} = \frac{C_{ex}}{C_0} \times 100\% \quad (1)$$

where  $C_{ex}$  represents the concentration of extracted  $\text{Hg}^{2+}$  and  $C_0$  refers to the initial concentration of  $\text{Hg}^{2+}$  used for the extraction.

### 2.5. Determination of the performance of PVP@MNP based DmSPE in real sample analysis

The optimized PVP@MNP based method was used to determine  $\text{Hg}^{2+}$  in drinking water, mineral water, and surface water. The surface water was collected from the lake around Kuala Lumpur, Malaysia. The selected water samples were filtered through the 0.45  $\mu\text{m}$  membrane filter. These water samples were free from  $\text{Hg}^{2+}$ . Consequently, these water samples were spiked with the known concentration of  $\text{Hg}^{2+}$ .  $\text{Hg}^{2+}$  in water samples was pre-concentrated with the optimized DmSPE conditions: pH 7, 10 mg of PVP@MNP, 60 min agitation for extraction, 0.5 mL of desorption reagent (2% thiourea in 0.1 M HCl (TUA-HCl)), and 5 min of agitation for desorption.

### 3. Results and Discussion

#### 3.1. PVP@MNP characterization

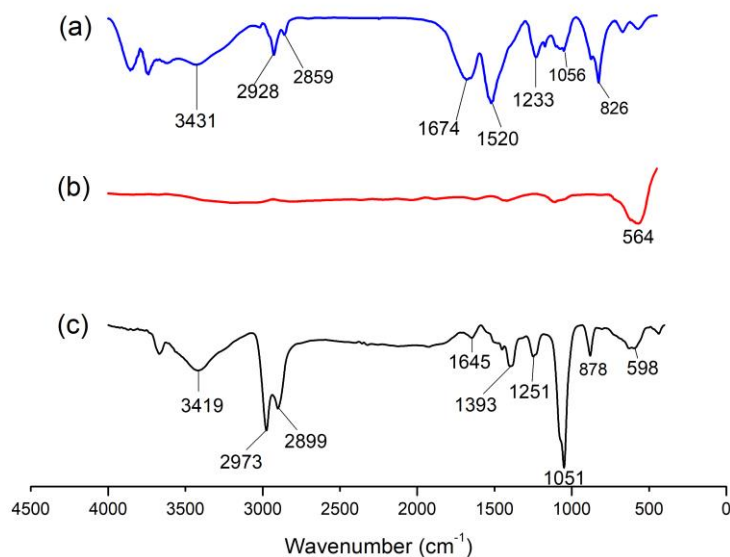


**Figure 1.** FTIR spectra of (a) PVP, (b) MNP and, (c) PVP@MNP

FTIR analysis was carried out to confirm the presence of PVP on MNP after the coating process. Figure 1 shows the FT-IR spectra of MNP, PVP, and PVP@MNP. FTIR spectrum of MNP showed a significant peak at  $564\text{ cm}^{-1}$ , indicating the presence of Fe-O (Lesiak et al., 2019). PVP shows the peaks at 3431 and  $2800\text{--}2900\text{ cm}^{-1}$  were due to OH stretching and C-H stretching of the aromatic ring, respectively (Zhang et al., 2017). PVP also shows a peak at  $1674\text{ cm}^{-1}$  due to the C-H bending of the aromatic ring. The peak at  $1233\text{ cm}^{-1}$  indicates the presence of the C-O bond in PVP. The emergence of the peaks from both PVP (3419, 2973, 2899,  $1645\text{ cm}^{-1}$ ) and MNP ( $598\text{ cm}^{-1}$ ) in PVP@MNP suggesting PVP was successfully coated on MNP. To further confirm this result, elemental analysis was performed on the MNP and PVP@MNP. The PVP@MNP showed the presence of 22.2% of carbon. In contrast, carbon was not detected in MNP (Table 1). This result further indicated that the PVP@MNP was successfully synthesized. Figure 2 shows the SEM image of MNP and PVP@MNP. There are no significant changes in the morphology after coating. Both MNP and PVP@MNP showed spherical shapes. The size of the PVP@MNP was ranged from 11 – 23 nm, which is slightly larger

than MNP with the size ranging from 7 – 15 nm. This result could be useful to further indicate the presence of PVP on the MNP.

**Table 1.** Elemental composition of MNP and PVP@MNP.

Element	Percentage (%)	
	MNP	PVP@MNP
Fe	60.3	26.6
O	39.7	51.2
C	0	22.2

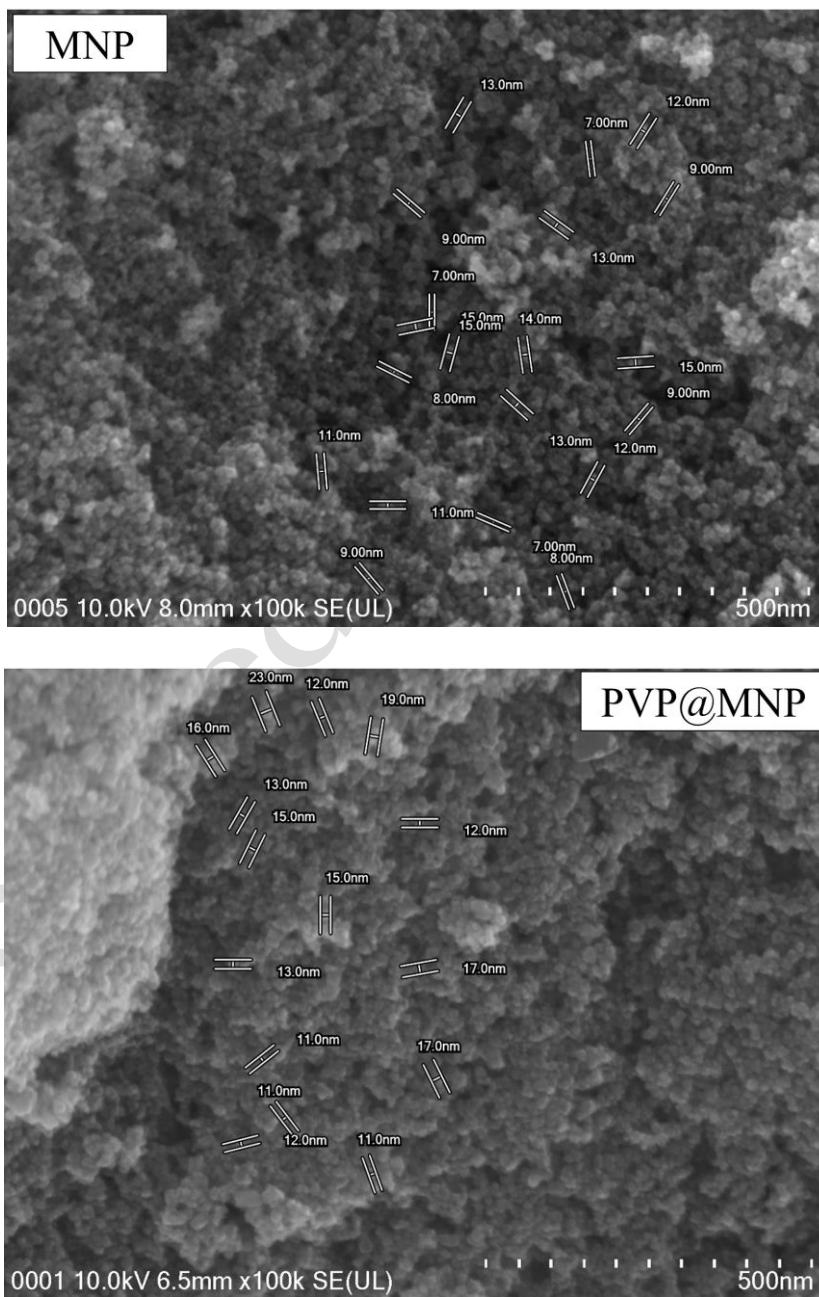


**Figure 2.** Scanning electron microscope image of MNP and PVP@MNP

### 3.2. Optimization of PVP@MNP based DmSPE

In general, the amount of sorbent plays a huge influence in the adsorption of analytes in the DmSPE process. The sorbent dosage determines the surface area and the number of active sites for the adsorption (Ghodsi et al., 2021). In order to obtain the maximum adsorption efficiency, the impact of the amount of PVP@MNP was investigated in the range of 10 to 40 mg. the percent removal was slightly increased from 82.3 to 96.8% when the amount of PVP@MNP was increased from 10 to 40 mg (Figure 3a). However, this increment was found to be insignificant. Therefore, for further studies, 10 mg of PVP@MNP was selected to reduce sorbent usage. The dispersion of the PVP@MNP was performed using an orbital shaker at room temperature. Consequently, the agitation time was investigated to ensure the PVP@MNP was dispersed effectively in the water for achieving the most efficient  $\text{Hg}^{2+}$  adsorption. The percent removal of  $\text{Hg}^{2+}$  was increased significantly to 93.4% at the 10 min of adsorption time (Figure 3b). The percent  $\text{Hg}^{2+}$  removal was increased to 95.9% at 30 min of agitation time. The result also showed that the percentage of  $\text{Hg}^{2+}$  removal was further increased to 98.6% at 60 min, and no significant improvement of  $\text{Hg}^{2+}$  removal was observed after 60 min. Consequently, 60 min of agitation time was chosen for further study to improve the adsorption efficiency of  $\text{Hg}^{2+}$  by PVP@MNP.

The pH of the solution influences the speciation of  $\text{Hg}^{2+}$  in water and the degree of ionization of PVP. To study the effect of pH on the  $\text{Hg}^{2+}$  removal, the pH of the solution was varied from 3 to 9. The percent removal of  $\text{Hg}^{2+}$  by PVP@MNP was 5.75% at pH 3. However, the percentage removal was increased significantly to 99.9% when the pH was varied from 4.0 to 9.0 (Figure 3c). At pH 3, the low removal efficiency of  $\text{Hg}^{2+}$  was because of the competition between  $\text{H}^+$  with  $\text{Hg}^{2+}$  and  $\text{Hg}(\text{OH})^+$  for the active sites of PVP@MNP (Abdallah *et al.*, 2020). When the pH was increased to pH 4, the phenol group of PVP was ionized to form negatively charged phenolate, which could interact favorably with  $\text{Hg}^{2+}$  via ionic interaction. As reported by Abdallah *et al.* (2020), water-soluble  $\text{Hg}(\text{OH})_2$  is the main species at pH 5 and above. The high removal efficiency of  $\text{Hg}^{2+}$  at high pH indicated that  $\text{Hg}(\text{OH})_2$  interacted favorably with PVP@MNP. At pH 7, the  $\text{Hg}^{2+}$  removal was found

to achieve 99.9%. Therefore, this pH condition was selected for the following experiment. The selection of pH 7 is also an advantage for environmental analysis because pH adjustment is not required.

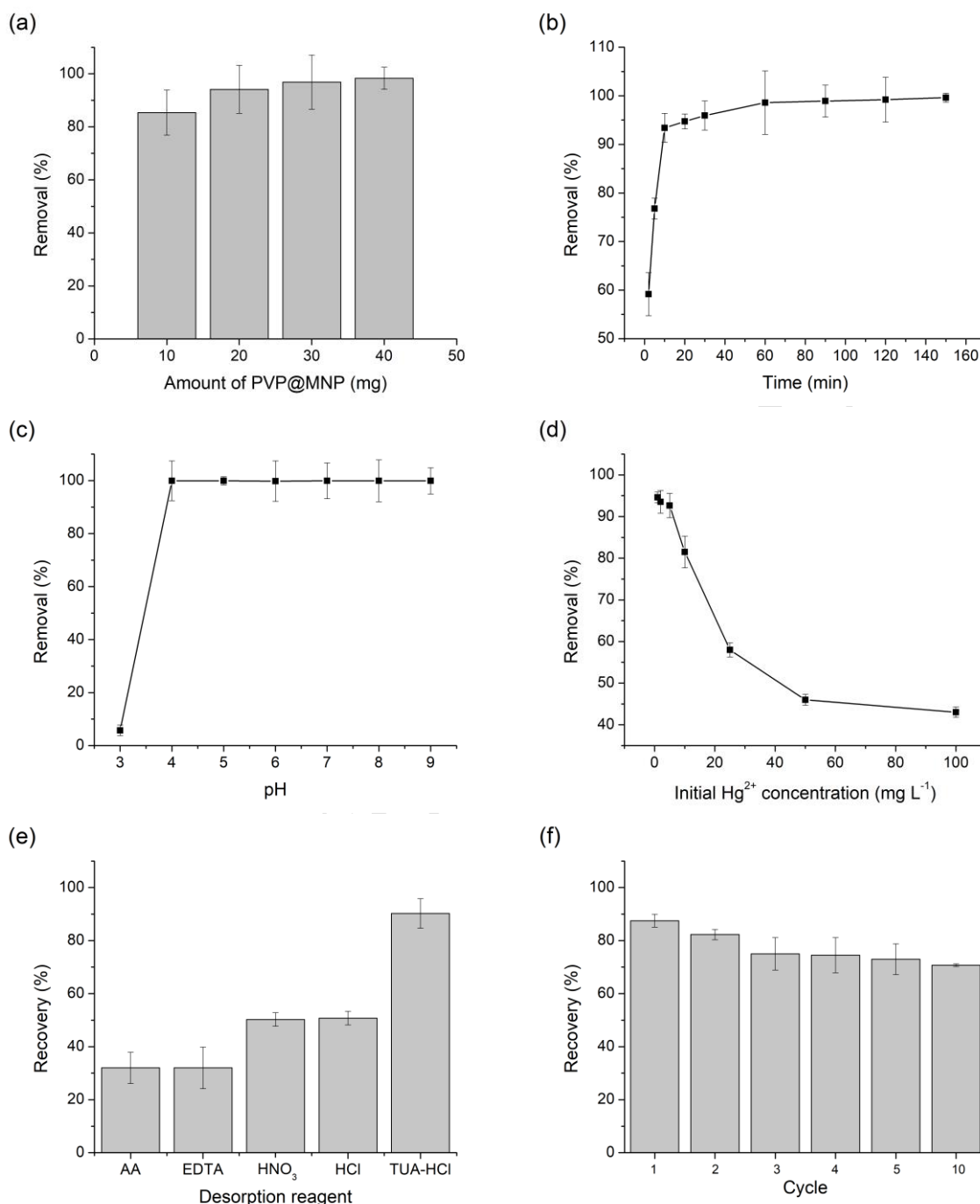


**Figure 3.** The influence of (a) the amount of PVP@MNPs ( $[Hg^{2+}] = 1\ mg\ L^{-1}$ , volume of  $Hg^{2+}$  solution = 20 mL, pH = 7 and adsorption time = 60 min), (b) adsorption time (Amount of adsorbent = 10 mg,  $[Hg^{2+}] = 1\ mg\ L^{-1}$ , pH = 7 and volume of  $Hg^{2+}$  solution = 20 mL), (c) pH (Amount of adsorbent = 10 mg,  $[Hg^{2+}] = 1\ mg\ L^{-1}$ , volume of aqueous solution = 20 mL and adsorption time = 60 min), (d)  $Hg^{2+}$  concentration (Amount of adsorbent = 10 mg, volume of aqueous solution = 20 mL, adsorption time = 60 min and pH of aqueous solution = 7) on the removal of  $Hg^{2+}$  in aqueous sample, (e) different desorption reagents on the recovery of  $Hg^{2+}$  from PVP@MNP and (f) Reusability of PVP@MNP.

The experiment for the effect of  $\text{Hg}^{2+}$  concentration showed that when the concentration of  $\text{Hg}^{2+}$  was increased from 0.5 to 10  $\text{mg L}^{-1}$ , the percentage of  $\text{Hg}^{2+}$  removal by PVP@MNP was decreased from 97.0 to 81.5% (Figure 3d). The effectiveness of  $\text{Hg}^{2+}$  adsorption was found to diminish further from 81.5 to 43.0 % with increasing concentration of  $\text{Hg}^{2+}$  from 10 to 100  $\text{mg L}^{-1}$ . This observation was mainly due to the occurrence of a higher amount of  $\text{Hg}^{2+}$  in the solution when the concentration of  $\text{Hg}^{2+}$  increased. However, the available active sites for the adsorption of  $\text{Hg}^{2+}$  remained constant when the amount of PVP@MNP was fixed (Al-Ghouti *et al.*, 2019).

For searching the most effective reagent to desorb the  $\text{Hg}^{2+}$  from PVP@MNP, the performance of 0.1 M acetic acid ( $\text{CH}_3\text{COOH}$ ), 0.1 M ethylenediaminetetraacetic acid (EDTA), 0.1 M nitric acid ( $\text{HNO}_3$ ), 0.1 M hydrochloric acid (HCl), and 2% thiourea in 0.1M HCl solution (TUA-HCl) were evaluated. These reagents have the ability to solubilize metal ions (Alguacil *et al.*, 2020). The desorption process was carried out by agitating the PVP@MNP loaded with  $\text{Hg}^{2+}$  with 0.5 mL of the selected desorption reagents. According to Figure 3e, TUA-HCl shows the highest efficiency in extracting  $\text{Hg}^{2+}$  from PVP@MNP. TUA-HCl is usually utilized to desorb  $\text{Hg}^{2+}$  ions from sorbents because the sulfur and nitrogen atoms in thiourea have a strong affinity to complex with  $\text{Hg}^{2+}$ . Also, chloride ions from HCl could complex with the  $\text{Hg}^{2+}$  and result in the formation of  $\text{HgCl}_2$  (Velempini *et al.*, 2019).

The reusability of a sorbent is a significant factor to consider when deciding on the sustainability of analytical method (Fu *et al.*, 2017). Ten cycles of adsorption-desorption were carried out continuously on a single adsorbent sample, and the results are shown in Figure 3f. Considering the  $\text{Hg}^{2+}$  in the real environment is far lower than 1 ppm, PVP@MNP could be reused. PVP@MNP for ten consecutive adsorption cycles (Alinezhad *et al.*, 2020). The adsorption property of PVP@MNP showed only a slightly decreased after ten cycles of adsorption-desorption 87.5 to 70.0% (Figure 3f).

### 3.3. Mechanism of the adsorption

The adsorption data were fitted to Langmuir and Freundlich isotherm models to understand how  $\text{Hg}^{2+}$  is adsorbed by PVP@MNP (Naushad *et al.*, 2019). Langmuir model describes the monolayer adsorption of sorbate by homogenous active sites of the sorbent (Bushra *et al.*, 2019). The linearized form of the Langmuir model can be written as:

$$\frac{C_e}{Q_e} = \frac{1}{Q_m B_L} + \frac{C_e}{Q_m} \quad (2)$$

where  $C_e$  is the concentration of  $\text{Hg}^{2+}$  in water after reaching the equilibrium,  $Q_e$  represents the equilibrium adsorption capacity.  $Q_m$  is the maximum adsorption capacity, and  $B_L$  is the Langmuir constant related to the energy of adsorption.  $Q_e$  was calculated using Equation (3):

$$Q_e = \left( \frac{C_o - C_e}{m} \right) v \quad (3)$$

where  $C_o$  is the initial concentration of  $\text{Hg}^{2+}$ ,  $m$  represents the mass of PVP@MNP, and  $V$  is the volume of the  $\text{Hg}^{2+}$  solution. On the other hand, the Freundlich model describes the multilayer adsorption of sorbate on non-uniform active sites of the sorbent with a heterogeneous surface (Bushra *et al.*, 2019). The linearized form of the Freundlich model is given in Equation (4):

$$\log Q_e = \log B_F + \frac{1}{n} \log C_e \quad (4)$$

where  $B_F$  is the Freundlich constant related to adsorption capacity, and  $n$  represents the adsorption intensity constant. The coefficient of determination ( $R^2$ ) value of the Freundlich model was 0.987, which was higher than the Langmuir model with the  $R^2$  value of 0.838 (Figures 4a and b). This observation recommended that PVP@MNP adsorbed the  $\text{Hg}^{2+}$  via a multilayer adsorption process described by the Freundlich model. Table 2 shows the adsorption isotherm parameters for Langmuir and Freundlich model. The separation factor,  $R_L$ , was calculated to determine the favorability of the adsorption of  $\text{Hg}^{2+}$  by PVP@MNP using Equation 5. The adsorption process is defined as favorable if  $R_L$  values are fall within 0 to 1. The adsorption process is unfavorable or linear if values are larger

than 1 or equal to 0, respectively. The  $R_L$  values obtained for this study was ranged from 0.08 – 0.89 (Table 2), which indicated that the adsorption process of  $Hg^{2+}$  by PVP@MNP is favorable.

$$R_L = \frac{1}{1 + (B_L \times C_0)} \quad (5)$$

**Table 2** Adsorption isotherm parameters of Langmuir and Freundlich model.

Adsorption Isotherm Model	Parameter			
	$Q_m$ (mg/g)	$B_L$ (L/mg)	$R_L$	$R^2$
Langmuir	21.1	0.1199	0.08 - 0.89	0.8383
Freundlich	$B_F$ (L/mg)	$1/n$	$n$	$R^2$
	2.63	0.4969	2.01	0.9746

As mentioned in the previous section, the adsorption of  $Hg^{2+}$  by PVP@MNP is expected to proceed via complexation. Consequently, the data obtained were fitted to the pseudo-first-order and pseudo-second-order kinetic models. Pseudo-first-order kinetic model describes the physical adsorption that the adsorption rate is influenced by the number of available adsorption sites on the materials (Shojaeiarani et al., 2021). On the other hand, the pseudo-second-order model indicates the chemisorption between sorbate and adsorbent, including the exchange or transfer of valence electrons (Ho, 2006). The linearized form of pseudo-first-order and pseudo-second-order models can be described by Equation (6) and (7):

$$\log(Q_e - Q_t) = \log Q_e - \frac{k}{2.303} t \quad (6)$$

$$\frac{t}{Q_t} = \frac{t}{Q_e} + \frac{1}{KQ_e^2} \quad (7)$$

where  $Q_t$  is the amount of adsorbed sorbate at time  $t$ .  $k$  is the rate constant of the pseudo-first-order, and  $K$  is the pseudo-second-order rate constant. Figures 4c and d show that the data were well fitted to the pseudo-second-order with  $R^2$  near to 1. The  $R^2$  value of pseudo-first-order was 0.9238, which is lower than the pseudo-second-order. This result showed the adsorption of  $Hg^{2+}$  by PVP@MNP was mainly happened through chemisorption.

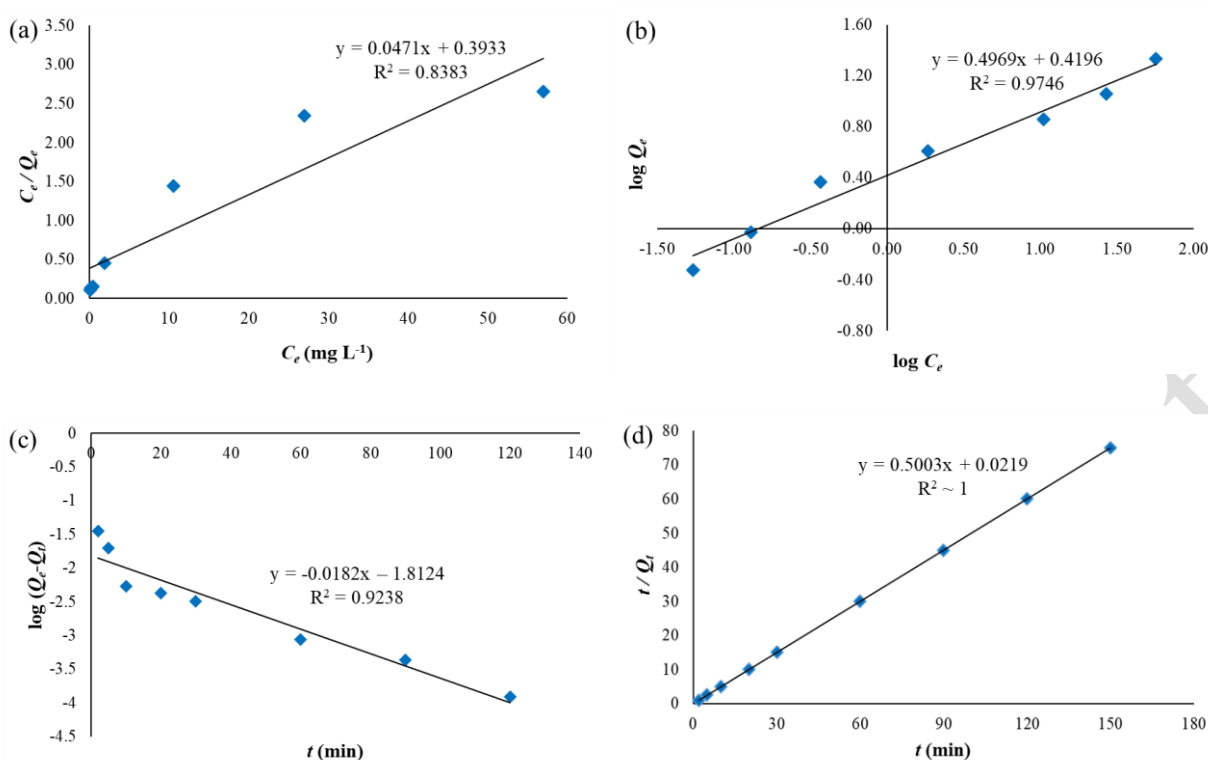


**Figure 4.** (a) Adsorption isotherm Langmuir model, (b) adsorption isotherm Freundlich model, and (c) Pseudo-second-order model for adsorption of  $\text{Hg}^{2+}$  on PVP@MNP.

### 3.4. Analytical performance of PVP@MNP based DmSPE in water analysis

The analytical performance of the optimized PVP@MNP based DmSPE method was assessed using linearity, the method detection limit (MDL), the limit of quantitation (LOQ), enrichment factor, inter-day, and intra-day precision. The enrichment factor (EF) was determined using the sample spiked with  $\text{Hg}^{2+}$  at  $1000 \mu\text{g L}^{-1}$ . EF value was obtained using the following equation:

$$EF = \frac{C_F}{C_0} \quad (6)$$

where  $C_0$  and  $C_F$  refer to the initial and final concentration of  $\text{Hg}^{2+}$ . The calculated EF value was 40. The optimized method showed a good correlation factor  $R^2$  near to 1 for the linear range of 100 to  $2000 \mu\text{g L}^{-1}$ . In this experiment, MDL and LOQ were determined by analyzing seven replicates of

deionized water spiked with  $\text{Hg}^{2+}$  at the concentration equal to signal to noise ratio of 5. MDL and LOQ were calculated using Equations (7) and (8):

$$MDL = S \times (t - value) \quad (7)$$

$$LOQ = S \times 10 \quad (8)$$

where  $S$  is the standard deviation of the concentration of  $\text{Hg}^{2+}$  obtained from the seven replicates of analysis. The  $t$ -value of 3.143, representing 99% of a confidence level, was used to calculate the MDL (Ripp, 1996). The obtained MDL and LOQ for the optimized method were 0.01 and 0.04  $\mu\text{g L}^{-1}$ , respectively

The intraday and interday reproducibility of the PVP@MNP based DmSPE was expressed in percent relative standard deviation (%RSD) by analyzing sets of four and five replicates, respectively. The %RSD obtained were ranged from 3.4-7.3% for intraday reproducibility and 1-5.1% for interday reproducibility. The analytical performance of the developed PVP@MNP based DmSPE was comparable with other reported DmSPE techniques in terms of detection limit and LOQ (Table 2). The developed method was also achieved lower detection limits than most of the reported studies. Therefore, it can be concluded that the developed method was an effective procedure for the preconcentration of  $\text{Hg}^{2+}$  in water.

**Table 2.** Comparison of the developed method with other DmSPE methods in the  $\text{Hg}^{2+}$  analysis.

Absorbent	Detection limit ( $\mu\text{gL}^{-1}$ )	LOQ ( $\mu\text{gL}^{-1}$ )	Reference
Dendrimer functionalized magnetic nanosorbent	0.03	Not reported	Ghodsi <i>et al.</i> , 2021
Ion-imprinted magnetic nanoparticle	0.084	0.28	Jiang <i>et al.</i> , 2017
1,5-diphenylcarbazine functionalized magnetic sorbent	0.16	Not reported	Zhai <i>et al.</i> , 2010
PVP@MNP	0.01	0.04	This study

For validation, drinking water, mineral water, and surface water spiked with  $\text{Hg}^{2+}$  at the concentration of 100, 500, and 2000  $\mu\text{g L}^{-1}$  were analyzed using the optimized method. The intraday and interday recovery and precision of the optimized method are presented in Table 3. The obtained recovery for  $\text{Hg}^{2+}$  was ranged from 72 to 90%, with the relative standard deviation of 1-5% for both the intra-day and inter-day precision, respectively. These results indicated that the matrices of the selected water samples do not significantly impact the performance of the developed method.

**Table 3** Recoveries of  $\text{Hg}^{2+}$  in the real water samples.

Sample	Spiked [ $\text{Hg}^{2+}$ ] ( $\mu\text{g L}^{-1}$ )	*RSD%	
		Inter-day (n=4)	Intra-day (n=5)
Drinking water	0	ND	ND
	100	75±1	76±2
	500	77 ± 1	76±1
	2000	83±3	84±4
Mineral water	0	ND	ND
	100	75±2	78±1
	500	79±1	79±1
	2000	78±1	90±5
Surface water	0	ND	ND
	100	72±1	85±1
	500	75±5	89±2
	2000	86±1	80±5

\* Experiments were carried out within 22 – 26 March 2021

#### 4. Conclusion

In this study, a magnetic adsorbent, PVP@MNP, was synthesized through a single-step coating method at room temperature. The PVP@MNP was then used as a sorbent to develop a DmSPE method for the analysis of  $\text{Hg}^{2+}$  in water. The developed PVP@MNP based DmSPE showed a low method detection limit at 0.01  $\mu\text{g L}^{-1}$  and LOQ at 0.04  $\mu\text{g L}^{-1}$ . This method also showed a wide range of linearity with good repeatability. The PVP@MNP was suitable for repeated use over ten cycles without significant loss in the initial adsorption capacity. This method also showed that the determination of  $\text{Hg}^{2+}$  in drinking water, mineral water, and surface water reached a recovery efficiency of 72 to 90% with low %RSD for intraday and interday reproducibility. In conclusion, this

performance of the developed PVP@MNP based DmSPE method is comparable with other reported DmSPE methods.

## Acknowledgments

This research was supported financially by the Ministry of Higher Education Malaysia (Fundamental Research Grant Scheme No. FP042-2016).

## References

- Abdallah S.A., Tay K.S., Low K.H. (2020), Feasibility of mercury (II) ion removal by nitrated polycarbonate derived from waste optical discs, *International Journal of Environmental Science and Technology*, **17**, 4161-4170.
- Al-Ghouti M.A., Da'ana D., Abu-Dieyeh M., Khraisheh M. (2019), Adsorptive removal of mercury from water by adsorbents derived from date pits, *Scientific Report*, **9**, 15327.
- Alguacil F.J., López F.A. (2020), Adsorption processing for the removal of toxic Hg(II) from liquid effluents: Advances in the 2019 year, *Metals*, **10**, 412.
- Alinezhad H., Zabihi M., Kahfroushan D. (2020), Design and fabrication the novel polymeric magnetic boehmite nanocomposite (boehmite@ Fe<sub>3</sub>O<sub>4</sub>@PLA@SiO<sub>2</sub>) for the remarkable competitive adsorption of methylene blue and mercury ions, *Journal of Physics and Chemistry of Solids*, **144**, 109515.
- Bushra R., Ahmed A., Shahadat M. (2017), Mechanism of adsorption on nanomaterials, In: *Advanced Environmental Analysis: Applications of Nanomaterials*, Hussain C.M. and Kharisov B. (Eds.), The Royal Society of Chemistry: London, UK.

- Chen Y., He M., Chen B., Hu B. (2021), Thiol-grafted magnetic polymer for preconcentration of Cd, Hg, Pb from environmental water followed by inductively coupled plasma mass spectrometry detection, *Spectrochimica Acta Part B: Atomic Spectroscopy*, **177**, 106071.
- Chisvert A., Cárdenas S., Lucena R. (2019), Dispersive micro-solid phase extraction, *Trends in Analytical Chemistry*, **112**, 226-233.
- Dibbern M., Elmeros M., Dietz R., Søndergaard J., Michelsen A. Sonne, C. (2021), Mercury exposure and risk assessment for Eurasian otters (*Lutra lutra*) in Denmark, *Chemosphere*, **272**, 129608.
- Fu Y., Chen Z., Ying S., Wang J., Hu J. (2017) Functionalized magnetic mesoporous silica/poly(m-aminothiophenol) nanocomposite for Hg(II) rapid uptake and high catalytic activity of spent Hg(II) adsorbent, *Science of the Total Environment*, **574**, 1379-1388.
- Ghodsi S., Behbahani M., Badi M.Y., Ghambarian M., Sobhi H.R., Esrafil A. (2021), A new dendrimer-functionalized magnetic nanosorbent for the efficient adsorption and subsequent trace measurement of Hg (II) ions in wastewater samples, *Journal of Molecular Liquids*, **323**, 114472.
- Ho Y. (2006), Review of second-order models for adsorption systems, *Journal of Hazardous Materials*, **136**, 681-689.
- Imran U., Mahar, R.B., Ullah, A. Shaikh, K. (2021), Seasonal Variability of Heavy Metals in Manchar Lake of Arid Southern Pakistan and Its Consequential Human Health Risk, *Polish Journal of Environmental Studies*, **30**, 163-175.
- Jiang W., Jin X., Yu X., Wu W., Xu L., Fu F. (2017), Ion-imprinted magnetic nanoparticles for specific separation and concentration of ultra-trace methyl mercury from aqueous sample, *Journal of Chromatography A*, **1496**, 167-173.
- Khor S.W., Lee Y.K., Tay K.S. (2019), Selective magnetic mercury(II) ion capturing ligand-doped silica gel for water analysis, *Analyst*, **144**, 1968–1974.

- Lesiak B., Rangan N., Jiricek P., Gordeev I., Tóth J., Kövér L., Mohai M., Borowicz P. (2019) Surface study of Fe<sub>3</sub>O<sub>4</sub> nanoparticles functionalized with biocompatible adsorbed molecules, *Frontiers in Chemistry*, **7**, 642.
- Ma J., Wang H., Zhang M., Li D., Liu L., Yang H. (2020), Preparation of terpyridine-functionalized paramagnetic nickel–zinc ferrite microspheres for adsorbing Pb(ii), Hg(ii), and Cd(ii) from water, *RSC Advances*, **10**, 39468.
- Marrugo-Negrete J., Pinedo-Hernández J., Marrugo-Madrid S., Díez S. (2021), Assessment of trace element pollution and ecological risks in a river basin impacted by mining in Colombia, *Environmental Science and Pollution Research*, **28**, 201-210.
- Naushad M., Ahamad T., AlOthman Z.A., Al-Muhtaseb A.H. (2019), Green and eco-friendly nanocomposite for the removal of toxic Hg(II) metal ion from aqueous environment: Adsorption kinetics & isotherm modelling, *Journal of Molecular Liquids*, **279**, 1-8.
- Pokhrel L.R., Ettorre N., Jacobs Z.L., Zarr A., Weir M.H., Scheuerman P.R., Kanel S.R., Dubey B. (2017), Novel carbon nanotube (CNT)-based ultrasensitive sensors for trace mercury(II) detection in water: A review, *Science of the Total Environment*, **574**, 1379-1388.
- Ripp J. (1996), Analytical detection limit guidance & laboratory guide for determining method detection limits, Wisconsin Department of Natural Resources: Laboratory Certification Program.
- Shirani M., Afzali K.N., Jahan S., Strezov V., Soleimani-Sardo, M. (2020), Pollution and contamination assessment of heavy metals in the sediments of Jazmurian playa in southeast Iran, *Scientific Report*, **10**, 4775.
- Shojaeiarani J., Shirzadifar A., Bajwa D.S. (2021) Robust and porous 3D-printed multifunctional hydrogels for efficient removal of cationic and anionic dyes from aqueous solution, *Microporous and Mesoporous Materials*, **327**, 111382.

Velempini T., Pillay K., Mbianda X.Y., Arotiba O.A. (2019), Carboxymethyl cellulose thiol-imprinted polymers: Synthesis, characterization and selective Hg(II) adsorption, *Journal of Environmental Sciences*, **79**, 280-296.

Zhai Y., He Q., Yang X., Han Q. (2010), Solid phase extraction and preconcentration of trace mercury (II) from aqueous solution using magnetic nanoparticles doped with 1,5-diphenylcarbazide, *Microchimica Acta*, **169**, 353-360.

Zhang G., Kim C., Choi W. (2017), Poly(4-vinylphenol) as a new stable and metal-free sensitizer of titania for visible light photocatalysis through ligand-to-metal charge transfer process, *Catalysis Today*, **281**, 109-116.

accepted manuscript